



Recovery of Benthic Microalgal Biomass and Community Structure Following Beach Renourishment at Folly Beach, South Carolina

Kristina M. Hill-Spanik¹ · Aubrey S. Smith^{1,2} · Craig J. Plante¹

Received: 26 February 2018 / Revised: 30 August 2018 / Accepted: 31 August 2018 / Published online: 8 October 2018
© Coastal and Estuarine Research Federation 2018

Abstract

One method of preserving beaches against the effects of erosion and sea level rise is beach renourishment. While there have been many studies assessing the impact of renourishment on macrofauna, few studies have looked at its effects on microbes. Benthic microalgae (BMA) are important primary producers, representing the basis of nearshore food webs. BMA also secrete extracellular polymeric substances (EPS), which bind sediment and thus help prevent erosion. The objective of this study was to monitor recovery of BMA in terms of relative biomass (estimated as sediment chlorophyll *a*) and community structure (characterized using high-throughput DNA sequencing) following renourishment of Folly Beach, SC in 2014. We also examined the relationships among biomass, EPS, and erosion. Sediment samples were collected intermittently ($n = 9$) from two renourished and two control sites within three intertidal zones (high, mid, low) from June 2014 to January 2015. Biomass recovered in sequence from low to high intertidal, corresponding to when the artificially-raised beach once again experienced regular tidal inundation (between 93 and 169 days post-renourishment). Alpha diversity metrics misleadingly indicated recovery around this same time within the high intertidal, but compositional changes through time were unlike those seen in control samples, and these communities had yet to recover at ~ 7 months post-renourishment. Renourishment therefore appears to impact BMA communities via artificial elevation of the beach face. While there were relationships between chl *a*, EPS, and erosion, BMA most likely play a minimal role in sediment stabilization in high-energy environments like Folly Beach.

Keywords Benthic microalgae · Microphytobenthos · Beach nourishment · High-throughput sequencing · South Carolina · Erosion · Extracellular polymeric substances

Introduction

Beach renourishment has been applied to reduce the effects of erosion along the U.S. Atlantic coast since 1923 (Valverde et al. 1999). While it is considered to be a better option both economically and ecologically compared to hard structures (Speybroeck et al. 2006), renourishment can change granulometric character and beach morphology (Speybroeck

et al. 2006), thus impacting beach ecosystems. These impacts have varied greatly—from negative to positive to unclear (Cahoon et al. 2012). Studies conducted to better understand the impacts of beach renourishment have mainly focused on macrofauna, sea turtles, fish, and shorebirds (for summary see Peterson and Bishop 2005), while little has been done to assess how renourishment affects primary producers (but see Cahoon et al. 2012, Snigirova 2013).

Benthic microalgae (BMA) are essential primary producers in nearshore intertidal and shallow, subtidal habitats (MacIntyre et al. 1996), e.g., contributing up to 50% of primary productivity in estuaries (Underwood and Kromkamp 1999). They also secrete extracellular polymeric substances (EPS) that bind sediment particles (Decho 1990; Underwood et al. 1995), which many studies have shown to increase resistance to erosive conditions (e.g., Holland et al. 1974; Madsen et al. 1993; Yallop et al. 2000). Correlations between BMA biomass, EPS production, and sediment grain size have been found, and interestingly, sediment armoring by EPS can increase the stability of sediment ten-fold (Tolhurst et al. 2003; Lubarsky et al. 2010).

Communicated by Deana Erdner

Electronic supplementary material The online version of this article (<https://doi.org/10.1007/s12237-018-0456-x>) contains supplementary material, which is available to authorized users.

✉ Kristina M. Hill-Spanik
hillkm1@cofc.edu

¹ Department of Biology, Grice Marine Laboratory, College of Charleston, Charleston, SC 29412, USA

² Medical University of South Carolina, Charleston, SC 29425, USA

Studies also have shown that BMA composition can affect the quantity and structure of the EPS produced (Stal 2010). BMA productivity and community composition has been extensively studied in estuaries and tidal flats (Underwood & Kromkamp 1999), but very few studies have examined productivity of BMA in sandy beach habitats, with even fewer examining those exposed to open-ocean conditions (but see e.g., Snigirova 2013 (Ukraine), Cahoon et al. 2012 (NC, USA), McLachlan et al. 1981 (South Africa); Nilsson 1995 (Sweden); Sousa and David 1996 (Brazil); Steele and Baird 1968 (Scotland)). Further, very little is known regarding the role of BMA and EPS in these higher-energy environments, and more specifically, whether EPS is providing stabilization of sediments here as in estuaries.

Our main objective was to assess BMA community recovery in terms of biomass (estimated as chlorophyll *a* (chl *a*)) and community structure following a renourishment event. Further, we wanted to determine if recovery differed within the intertidal zone given the different physical and granulometric characteristics of high, mid, and low intertidal environments. Secondly, we wanted to examine the relationships among BMA, EPS, and sediment stability in sandy sediments since one of the main reasons for beach renourishment is to reverse the effects of erosion. To address these objectives, we collected sediment intermittently from June 2014 to January 2015 from Folly Beach, South Carolina (SC), USA following a renourishment event and measured chl *a*, EPS, erosion/deposition, performed granulometric analyses, and assessed BMA community structure using high-throughput DNA sequencing.

Based on the high dispersal ability and short generation time of BMA, we expected recovery of biomass to occur relatively quickly (within days to weeks). We expected that renourishment would cause a decrease in diversity due to the burial of existing populations, but through time, communities would be reestablished and diversity restored. We also expected that the community composition from the renourished sites would differ from those of the controls initially, but recovery would be indicated by the communities becoming more similar through time. To our knowledge, this is the first study to examine the impacts of beach renourishment on BMA community structure using molecular methods, and it also provides baseline chl *a* and EPS data for SC beaches as these have not been described previously.

Materials and Methods

Sampling Sites and Collection

This study was conducted on Folly Island, which is a barrier island ~14 km south of Charleston, SC and is bounded by Lighthouse Inlet to the northeast and Stono Inlet to the southwest (Fig. 1). The mean tidal range for Folly Island is 1.6 m,

and the average wave height is 0.6 m (0.2 to 2.5 m) (Levine et al. 2009). The beach is gently sloped so that waves, which predominantly come from the northeast, inundate the beachfront at a low angle of incidence, and produce a south-southwest longshore current (Levine et al. 2009). Between January and June 2014, 1.1 million m³ of sand was deposited along 8.6 km of Folly Beach (Fig. 1; City of Folly Beach 2015) starting near the northeast end of the island and progressed to the southwest. The sediment was excavated using a hydraulic cutter head dredge from borrow sites 4.8 km offshore at a depth of 8.8 to 13.4 m and transported onto the beachfront via pipeline (USACE 2013). Bulldozers then leveled the beach face. Because there was restricted access to the renourished zones, we were unable to ascertain the exact time a zone had been completed (from deposition to leveling). Therefore, our sampling, which began on June 12, 2014, was somewhere between 3 and 5 days after renourishment—the earliest we could access the renourished zone. Four total sites were chosen for sampling: two within the renourished zone (R1 and R2) and two within areas that were not renourished to serve as controls (C1 and C2; Fig. 1). Again, because we had limited access to construction zones, which were ~150-m wide, it was necessary to space the R1 and R2 transects 100 m apart in order to ensure we sampled replicates at the same time interval after renourishment. Selection of C1 and C2 was restricted to two narrow swaths of unaltered beach on opposite ends of the island, because renourishment had taken place just a year earlier in May–June 2013 on the southwest end of the beach at Folly Beach County Park (City of Folly Beach 2015). C1 and C2 were ~100 m outside the renourished zone (Fig. 1).

Vertical transects ~100-m long for each site were situated perpendicular to the shore (Fig. 2). Sampling took place at 0 (just below the wrack line or “high” intertidal zone), 50

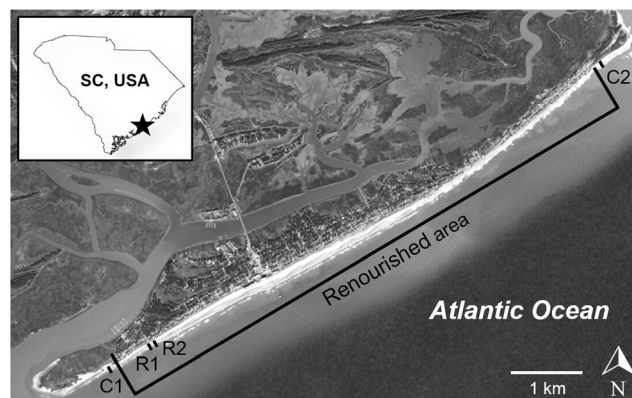


Fig. 1 Google Earth aerial view of Folly Beach, South Carolina (SC). Bracketed area indicates the portion that was renourished January to June 2014. Bold crossbars indicate the location of our sampling transects and sites. C = control, R = renourished. Source: Esri, DigitalGlobe, GeoEye, i-cubed, USDA, USGS, AEX, Getmapping, Aerogrid, IGN, IGP, swisstopo, and the GIS User Community

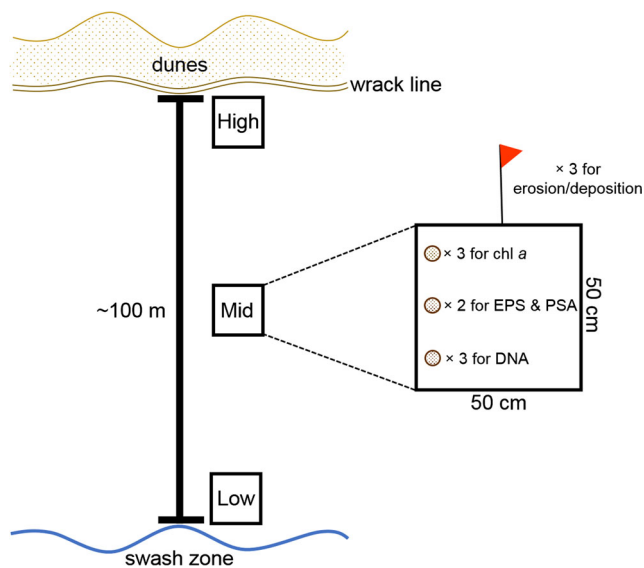


Fig. 2 Schematic of each of the four sampling sites (two renourished and two control). A 100-m transect (I-bar) was laid perpendicular to the shoreline starting just below the wrack line and ending just above the swash zone at low tide. Samples (circles) were randomly collected within a 50 × 50-cm quadrat (squares) from three intertidal zones (high, mid, low) between July 2014 and January 2015: three samples for chlorophyll *a* (chl *a*) quantification, two samples for extracellular polymeric substance (EPS) quantification and particle size analysis (PSA), and three samples for high-throughput DNA sequencing (DNA). Three erosion pins (flag) were also placed at each quadrat to measure erosion/deposition at each site (except for the second control site because of logistical constraints)

(“mid”), and 100 m (just above the swash zone at low tide or “low”) along the transect at each site (Fig. 2). At the first sampling time, PVC pipe was used to mark each site so that the same sites and their respective intertidal zones were sampled through time. Approximate tidal elevations of each intertidal zone at each site were determined by comparing tidal inundation times for Folly Island (outer coast) on NOAA’s Tides and Currents webpage (www.tidesandcurrents.noaa.gov) in July 2014 following the renourishment event and can be found in Supplementary Table 1. Our intention was for the zones to be equal at each site, but elevations at the renourished sites were inevitably higher due to deposited sand. Sediment samples were collected randomly within a 50 × 50-cm quadrat using a 10-cc syringe with the Luer-end cutoff. Each sample contained ~1 cm³ of the top 1 cm of sediment and was placed on ice until returned to the lab. Samples taken for chl *a* ($n = 3$) were then placed at -20 °C, and samples for molecular analyses ($n = 3$) were placed at either -20 or -80 °C until processing. Samples taken for EPS quantification ($n = 2$) were placed at 4 °C overnight for processing the following day.

Sites were resampled until chl *a* concentrations were similar (within 0.025- μg chl *a* g⁻¹ dry sediment) at all sites and resampled once more, with a total of nine sampling times: June 11–12, June 16–17, June 23–24, July 10 and 14, August

12–13, September 7 and 9, October 7 and 9, November 22 and 24, 2014, and January 21, 2015 corresponding to approximately 3, 9, 16, 36, 66, 93, 121, 169, and 230 days post-renourishment. It was necessary to sample over a 2-day period in all cases except the last because of the tide, distance between C2 and the other sites, and limited personnel. There were no major storms or flooding events during the sampling period. Sediment temperature was taken at each intertidal zone at each site for all sampling times, and wind speed data were accessed from an offshore buoy (Station FBIS1 located at 32° 41' 6" N 79° 53' 18" W) maintained by the National Data Buoy Center (http://www.ndbc.noaa.gov/station_page.php?station=fbis).

Erosion/Deposition

Sediment erosion and deposition were measured for all sampling times as in Thistle et al. (1995). Three erosion pins were spaced 0.5 m apart at each intertidal zone (high, mid, low) at each site except for C2. Metal pins (~0.1-cm thick, 500-mm long) were inserted normal to the sediment surface ~300-mm deep up to a labeled zero point. A small metal washer (0.1-cm thick, 0.95 cm in diameter with a 0.5-cm diameter hole in the center) was then placed around the pin such that the washer was flush with the sediment at the zero point. After ~24 h, net erosion/deposition was measured from the sediment level to the zero point, and maximum (max) erosion was measured from the position of the washer to the zero point.

Quantification of Chl *a*

For all sampling times, three samples from each intertidal zone at each site were extracted in HPLC-grade acetone. To estimate BMA biomass, chl *a* was quantified using a fluorometer (TD-700; Turner Designs, Inc. Sunnyvale, CA, USA) according to the Welschmeyer (1994) non-acidification method. Sediment was then rinsed with deionized water ~3 times to remove salts, dried at 65 °C for >48 h, and weighed to calculate μg chl *a* g⁻¹ dry sediment.

Quantification of EPS

EPS was extracted as in Hernandez et al. (2014) from two sediment samples from each intertidal zone at each site for all sampling times. Briefly, ~2–3-g sediment from each sample was incubated in 0.5-mM EDTA for 15 min at 40 °C with gentle shaking every 5 min, three consecutive times. Following each incubation, samples were centrifuged at 8000 ×g, and the supernates were pooled. Cold ethanol (4 °C) was mixed with the supernate so that the final concentration was 70% and then placed at 4 °C overnight to precipitate extracted EPS. Samples were centrifuged at 8000 ×g to collect the precipitate, which was then dissolved in 1 ml of deionized water, and used for quantification of EPS by the phenol-

sulfuric acid method. Absorbance was measured using a Spectronic 601 spectrophotometer (Milton Roy, Rochester, NY, USA) at 490 nm, and the amount of carbohydrate present was determined by comparison to a D-glucose calibration curve. Sediment samples were rinsed, dried, and weighed as in the above chl *a* methods to calculate mg EPS g⁻¹ dry sediment.

Particle Size Analyses

Median grain size, percent silt-clay, percent shell hash, and inclusive graphic standard deviation (σ_1 , a measurement of particle sorting) based on 10 measurements per sample were characterized using a Malvern Mastersizer 3000 Laser Diffraction-Particle Size Analyzer (Malvern, UK) fitted with a red light laser ($\lambda = 632.8$ nm) and a blue light laser ($\lambda = 470$ nm) following the manufacturer's protocol. This instrument determines particle sizes between 0.01 and 3500 μm in diameter, and the resulting average size distributions are based on an average volume distribution. Water was used as a dispersant (refractive index = 1.330), the particle refractive index was 1.500, and the Mie scattering model was used. Two replicate samples that were previously used for EPS quantification were pooled to obtain ~5 g of sediment after dry weights were taken. All analyses included samples collected from only the high and low intertidal zones at five of the nine sampling times (3, 36, 93, 169, and 230 days post-renourishment) to correspond to the samples chosen for high throughput DNA sequencing (HTS; see below). Although the maximum particle size for the instrument is 3 mm in one dimension, we found that small shell hash (~2.8 mm) would clog the instrument. Therefore, all samples were sieved prior to analysis to remove particles greater than 1 mm, and the weight percent of > 1-mm particles in each sample was calculated (i.e., percent shell hash). For σ_1 , $\sigma_1 < 0.350\Phi =$ very well sorted, and $> 4.00\Phi =$ extremely poorly sorted (Folk and Ward 1957).

DNA Extractions

Two sediment samples from the high and low intertidal zones at each site for five of the nine sampling times (3, 36, 93, 169, and 230 days post-renourishment) were selected for subsequent library preparation and high-throughput sequencing (HTS). It was unfeasible to do HTS for all three intertidal zones and nine sampling times, so we selected the high and low zones because the mid zone had more variation with respect to elevation, and therefore tidal inundation, throughout the sampling period compared to the high and low. We chose to analyze the first and last sampling times and three times in between in order to capture changes throughout the entire sampling period. DNA was extracted using an E.Z.N.A Soil DNA Kit (Omega Bio-tek, Norcross, GA, USA) following the manufacturer's protocol with modifications to increase DNA yields as in Bézy et al. (2014). Samples were subjected to ~

2000 oscillations min⁻¹ for 5 min in a bead beater (Mini Beadbeater-8, Biospec Products, Bartlesville, OK, USA) and 3 freeze-thaw cycles (-20 and 70 °C for 30 min each) during the lysis step. Multiple (2–3) extractions were done for some samples that did not PCR-amplify initially and were subsequently pooled and concentrated to also increase DNA concentration.

Library Preparation

Amplicon libraries were generated using the Ion Amplicon Library Preparation (Fusion Method) protocol (Life Technologies, Grand Island, NY, USA). Primers D512for (5'-ATTCCAGCTCCAATAGCG-3') and D978rev (5'-GACTACGATGGTATCTAATC-3') were used to amplify a region of the small subunit ribosomal RNA (SSU rRNA) gene, which contains the V4 region, and were designed specifically for amplification and barcoding of diatoms (Zimmermann et al. 2011). The forward and reverse primers included a 5' tail for Ion Torrent sequencing (adapter A: 5'-CCATCTCATCCCTGCGTGTCTCCGAC-3', adapter TrP1: 5'-CCTCTCTATGGGCAGTCGGTGAT-3', resp.). The forward primer also contained the 4-bp library key, an individual barcode for each sample (Ion Xpress Barcode Adapter Nos. 1, 2, 4–41, Life Technologies), and a barcode adapter. Replicates from the same site collected from the same intertidal zone and time were given the same barcode based on preliminary denaturing gradient gel electrophoresis results (data not shown). A 50- μl total reaction contained 1 \times TaKaRa *Ex Taq* Buffer (Clontech, Mountain View, CA, USA), 0.2-mM dNTPs, 0.5 μM each primer, 0.025-U μl^{-1} TaKaRa *Ex Taq* DNA polymerase (Clontech), and 5 μl of DNA template. An initial denaturation at 94 °C for 2 min was followed by 32 cycles of denaturation at 94 °C for 30 s, annealing at 50 °C for 30 s, and extension at 72 °C for 30 s, and then by a final extension at 72 °C for 2 min. Products were mixed with GelRed (Biotium, Hayward, CA, USA), electrophoresed on 1% agarose gels, and visualized under UV light.

Individual libraries were purified using 0.8 \times Agencourt AMPure XP beads (Beckman Coulter, Brea, CA, USA) or a Qiagen QIAquick Gel Extraction Kit (Valencia, CA, USA) according to the manufacturers' protocols and were then sized and quantified using a Bioanalyzer 2100 and DNA 1000 kit (Agilent Technologies, Santa Clara, CA, USA). Eighty libraries (with 40 barcodes) were pooled in equal concentrations, and the pool was quantified, again using a Bioanalyzer 2100 and DNA 1000 kit. The pooled library was sent to the Medical University of South Carolina Proteogenomics Facility (Charleston, SC, USA) for further size selection using a BluePippin (Sage, Beverly, MA, USA) and sequencing on an Ion Torrent Personal Genome Machine using an Ion 314 v2 chip (Life Technologies).

Statistical Analyses

Sequencing data analyses were performed using Quantitative Insights into Microbial Ecology v 1.9.1 (QIIME; Caporaso et al. 2010a). Raw reads were first demultiplexed and filtered to remove sequences with quality scores less than 20 and for sequence lengths less than 300 and greater than 600 base pairs (bp). USEARCH v5.2.236 (Edgar 2010) was used to detect and remove chimeras using UCHIME (Edgar et al. 2011), filter singletons, and assign operational taxonomic units (OTUs) using a sequence similarity threshold of 98% based on the diatom phylogenies in Luddington et al. (2012). Representative sequences for each OTU were then chosen and compared to the Silva rRNA database version 128 (Quast et al. 2013) at 94% clustering identity using the RDP classifier to assign taxonomy to each representative sequence (Wang et al. 2007). Sequences were aligned using PyNAST (Caporaso et al. 2010b), filtered (gap filter threshold = 0.8; entropy threshold = 0.10), and an approximately-maximum-likelihood phylogenetic tree was generated using FastTree 2.1.3 (Price et al. 2010). The OTU table was rarefied (or subsampled) for subsequent alpha and beta diversity analyses based on the sample with the fewest sequences. The OTU table was also used to generate the relative abundance of each taxonomic group within each sample. Because the primers amplified some non-target taxa (e.g., metazoans and fungi), we filtered the data to only include the following groups that were detected in our samples: Archaeplastida (Chloroplastida, Rhodophyceae), Cryptophyceae (excluding *Goniomonas*), Closteriaceae, Haptophyta, Ochrophyta, Tubulinea, Centrohelida, Apicomplexa (excluding gregarines), Ciliophora, and Rhizaria.

Shannon-Wiener diversity (H'), the number of distinct OTUs (S), Heip's evenness (E ; Heip 1974), and Chao1 richness (Chao 1984) were calculated in QIIME. Weighted and unweighted UniFrac distance matrices (Lozupone and Knight 2005) were also generated in QIIME, and analyses of similarity (ANOSIM; Clarke 1993) were used to explore differences in community structure within and between samples from differing treatments, intertidal zones, and days post-renourishment. Resulting ANOSIM R values were interpreted as in Clarke and Gorley (2001); $R > 0.75$ = well separated, $R > 0.5$ = overlapping, but different, $R > 0.25$ = barely separable, and $R < 0.25$ = indistinguishable. Lastly, principal coordinate analyses (PCoA) were performed using QIIME and visualized using EMPERor (Vázquez-Baeza et al. 2013).

All other statistics were performed using either R statistical package (R Core Team 2013) or JMP Pro 12 (SAS, Cary, NC). Shapiro-Wilk tests were performed to test for normality, and the Levene test was used to test for equal variances. If data were normally distributed and had equal variances ($p > 0.05$), analyses of variance (ANOVA) and subsequent Tukey pairwise tests were performed. If data and the transformations of these data were found to be non-parametric ($p < 0.05$), Kruskal-Wallis

(KW) tests were performed and subsequent non-parametric comparisons were done using the Wilcoxon method for each pair. If there was no significant difference or variation between sites within a treatment (e.g., R1 v R2, C1 v C2), data from both sites were combined for subsequent analyses. Where applicable, the standard error of the mean was calculated and reported below. Spearman's ρ correlation and jackknife distances outlier analyses were also performed using JMP Pro 12.

Results

Erosion/Deposition

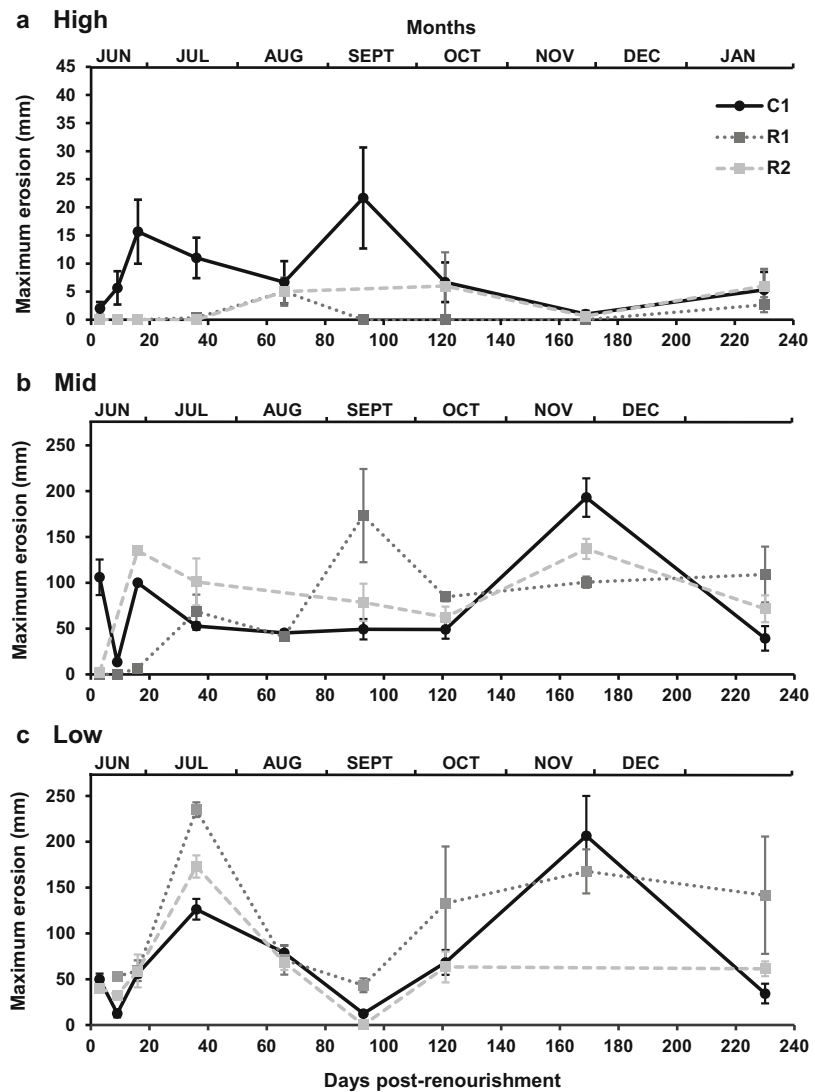
Overall, max erosion was significantly different among intertidal zones (high, mid, low) (KW $p < 0.0001$) and sampling times ($p = 0.003$), but not sites (C1, R1, R2). Net erosion/deposition varied significantly with respect to all variables ($p < 0.001$). There was more erosion (max and net) at the low and mid intertidal zones compared to the high ($p < 0.0001$), with no significant difference between the low and mid. There was less net erosion at C1 compared to both R1 and R2 overall ($p < 0.0001$). Mean max and net erosion/deposition for all sites at each intertidal zone can be found in Supplementary Table 1.

At the high intertidal zone, there were low levels of max and net erosion throughout, but erosion at the control and renourished sites were significantly different from one another ($p < 0.05$): C1 had greater max erosion compared to R1 and R2 ($p < 0.001$; Fig. 3a), but had less net erosion ($p < 0.05$). At the mid and low intertidal zones, there were clear temporal patterns with respect to erosion (Fig. 3b, c). At all of the low intertidal sites, there were distinct peaks in max erosion at 36 and 169 days post-renourishment (July and November; Fig. 3c); both times were significantly greater than all other sampling times ($p < 0.05$), but not significantly different from one another. At the mid intertidal zone, day 169 (November) also had significantly greater max erosion compared to all other sampling times ($p < 0.05$) except day 93 (September) (Fig. 3b). Net erosion followed a similar temporal pattern at the low and mid intertidal zones (data not shown).

Chlorophyll *a*

Average chl *a* varied significantly with respect to treatment (renourished, control), intertidal zone (high, mid, low), and sampling time (KW $p < 0.0001$ for all). There was significantly less chl *a* in sediments from the renourished treatment ($p < 0.0001$). Chl *a* peaked in August (66 days post-renourishment) and again in October (121 days post-renourishment) in samples from the control sites, while chl *a* in samples from the renourished sites peaked only once in September (93 days post-renourishment)—a month later

Fig. 3 Mean maximum erosion measurements taken 24 h after erosion pin deployment at the **a** high, **b** mid, and **c** low intertidal zones at the first control site (C1) and both renourished sites (R1 and R2) from June 2014 to January 2015. Note the difference in scale for the high intertidal zone. Error bars represent standard error



compared to the control sites (Fig. 4a). After September, chl *a* levels in sediments from both treatments were comparable and followed a similar temporal pattern (Fig. 4a).

Chl *a* concentrations were lowest in sediment from the high intertidal zone ($p < 0.0001$; Supplementary Table 1) where there was variation with respect to site (R1, R2, C1, C2; $p < 0.0001$) and sampling time ($p = 0.004$; Fig. 4b). Here, chl *a* in sediments from R1 and R2 were significantly different from one another (R1 > R2, $p = 0.003$). Sediment from C1 and C2 had comparable chl *a* levels, with both sites having significantly higher chl *a* when compared to the sediments from both R1 and R2 ($p \leq 0.0005$). Temporally, we saw a peak in chl *a* in sediment from all sites at 66 days post-renourishment (day 66 > 3, 16, 36, 66, 121, 169, $p < 0.05$; Fig. 4b).

Chl *a* in samples collected from the mid intertidal zone varied by treatment and sampling time ($p < 0.0001$ for both). The renourished samples had significantly less chl *a* than the control samples throughout the sampling period ($p < 0.010$; Fig. 4c; Supplementary Table 1). Average chl *a* values were

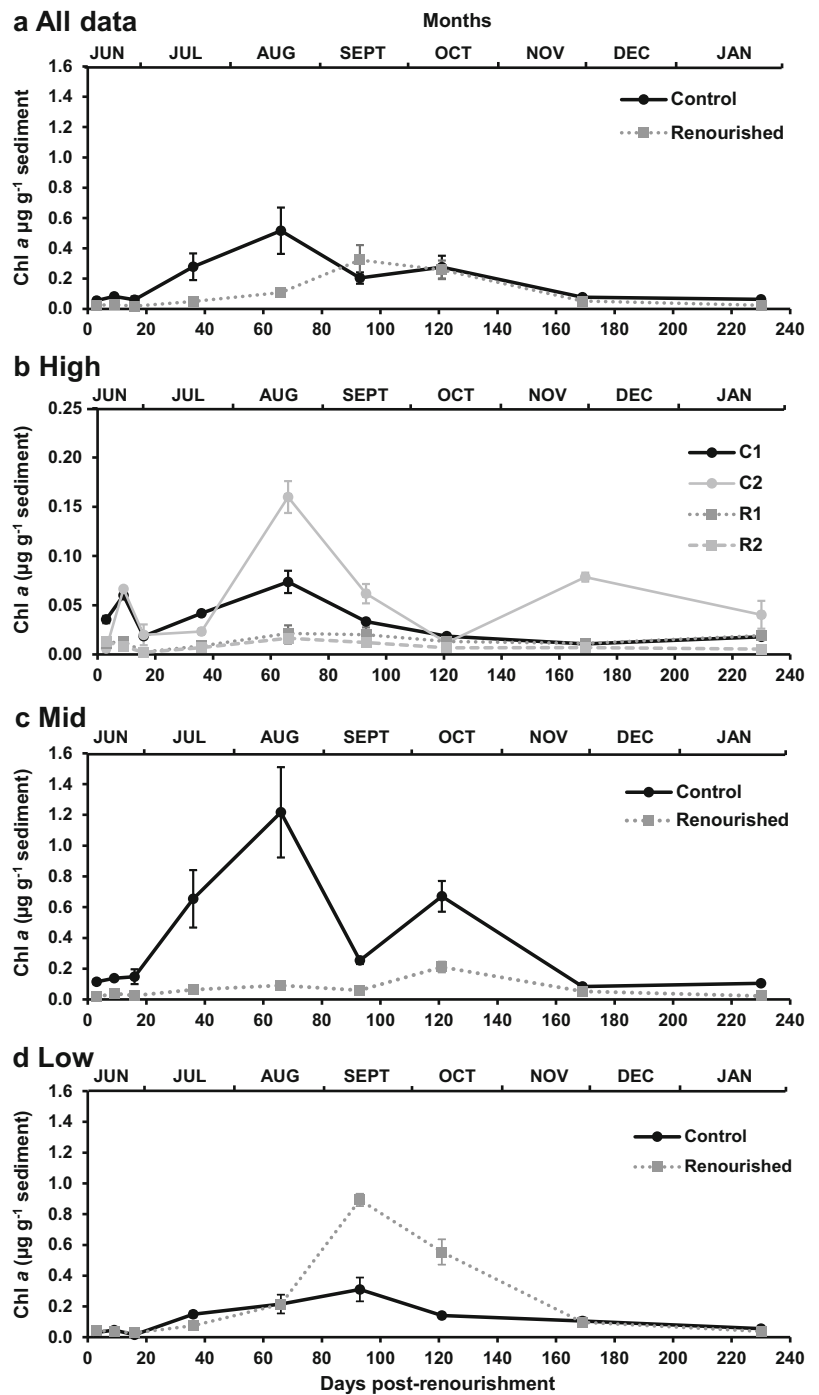
low in sediments from both treatments at 3 to 16 days post-renourishment (June), but peaked at 66 and 121 days post-renourishment (August and October) in control sediments (Fig. 4c). Chl *a* in renourished samples only had a small peak 121 days post-renourishment (October), after which chl *a* levels were again similar between treatments (Fig. 4c).

Chl *a* in samples collected from the low intertidal zone varied only by sampling time ($p < 0.0001$). Average chl *a* values in sediment from both treatments were low from 3 to 16 days post-renourishment (Fig. 4d) as we saw in those from the mid intertidal zone. The temporal pattern differed from the mid thereafter, with chl *a* levels increasing in both treatments to peak at 93 days post-renourishment, with higher levels in renourished samples (Fig. 4d).

EPS

Some EPS concentrations were undetectable (≤ 0), with no more than 0.061-mg g^{-1} dry sediment detected at all

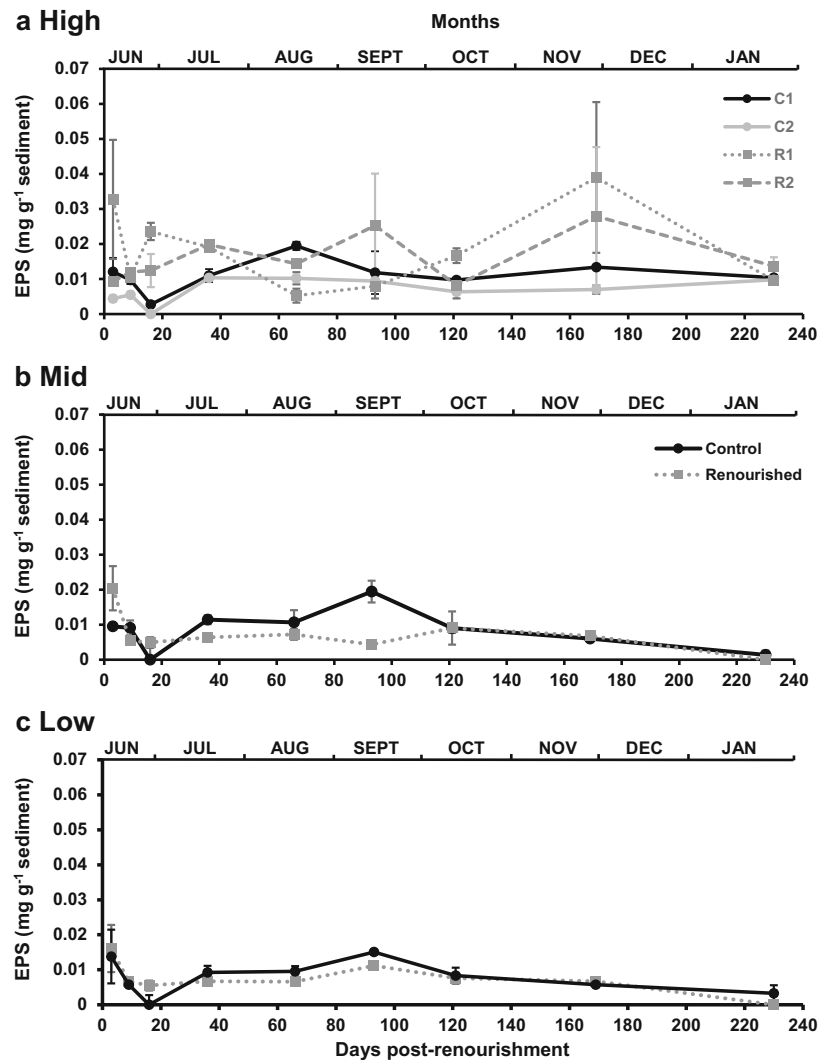
Fig. 4 Mean chlorophyll *a* ($\mu\text{g g}^{-1}$ dry sediment) in sediment collected from control and renourished sites from **a** all intertidal zones, and the **b** high, **c** mid, and **d** low intertidal zones from June 2014 to January 2015. All control (C1 and C2) and renourished (R1 and R2) sites are represented for the high intertidal zone because there was a significant difference between the two renourished sites; also note the difference in scale. Data from replicate sites were averaged for the mid and low. Error bars represent standard error



sites (R1, R2, C1, C2), intertidal zones (high, mid, low), and sampling times. EPS did not vary significantly by treatment, but did vary by intertidal zone and sampling time (KW $p < 0.0001$ for both). Sediment collected from the high intertidal zone had significantly higher EPS than mid and low intertidal samples ($p \leq 0.0002$; Supplementary Table 1).

EPS in high intertidal samples varied by site, with C2 samples having significantly less EPS compared to C1 ($p = 0.009$), R1 ($p = 0.0005$), and R2 samples ($p = 0.001$; Fig. 5a). There was no significant variation in EPS with respect to sampling time in high intertidal samples, but we did see variation through time in samples from both the mid and low intertidal zones ($p < 0.0001$ for both). The temporal

Fig. 5 Mean extracellular polymeric substance (mg g^{-1} dry sediment) in sediment collected from control and renourished sites from the **a** high, **b** mid, and **c** low intertidal zones from June 2014 to January 2015. All control (C1 and C2) and renourished (R1 and R2) sites are represented for the high intertidal zone because there was a significant difference between the two control site replicates. Replicate sites were averaged for the mid and low. Error bars represent standard error



pattern of EPS in sediments from these intertidal zones were very similar, peaking at 93 days post-renourishment in September and having less EPS on the final sampling date compared to other times (Fig. 5b, c). This pattern was seen in both treatments at the low intertidal, but was only seen in the control treatment in the mid intertidal. At the latter, the renourished treatment remained approximately the same throughout with the exception of 3 days post-renourishment when EPS concentration was the highest (Fig. 5b).

Particle Size Analyses

Median Grain Size

Median grain size varied significantly with respect to sampling time (ANOVA $p = 0.01$), but not treatment (renourished, control), intertidal zone (high, low), or the interactions of these variables overall. Means can be found in Table 1. Sediment samples collected from the high intertidal zone did not vary by treatment or intertidal zone. However, the renourished

samples had higher median grain size compared to control samples for most sampling times, though these differences were not significant (Supplementary Fig. 1a). Median grain size from low intertidal sediments varied by sampling time ($p = 0.002$), and the interaction of sampling time and treatment was marginally significant ($p = 0.053$). Here, sediment from the renourished treatment at 3 days post-renourishment (June) had significantly smaller median grain size compared to 230 and 169 days post-renourishment (November and January; $p < 0.01$; Supplementary Fig. 1b). Median grain size of sediments from the renourished treatment mirrors what was seen in the control (i.e., no significant change with respect to time) initially, but by November and January, median grain size of renourished samples exceeded that of the control. Median grain size of renourished samples at day 3 was also significantly smaller compared to control samples at day 230 (January; $p = 0.035$), while median grain size of control sediments did not vary significantly with respect to sampling time throughout (Supplementary Fig. 1b).

Table 1 Mean particle size analysis data \pm standard error of the mean for samples collected from the renourished and control sites at each intertidal zone (high and low). σ_1 = inclusive graphic standard

Intertidal zone	Treatment	Median grain size (μm)	% shell hash	% silt-clay	σ_1 (Φ)
High	Control	218.00 \pm 7.65	0.00 \pm 0.00	0.00 \pm 0.00	0.50 \pm 0.02
	Renourished	236.70 \pm 8.51	3.63 \pm 0.49	0.01 \pm 0.00	0.81 \pm 0.04
Low	Control	227.80 \pm 7.40	0.23 \pm 0.17	0.00 \pm 0.00	0.59 \pm 0.03
	Renourished	223.30 \pm 13.12	0.67 \pm 0.38	0.01 \pm 0.01	0.61 \pm 0.03

Percent Silt-Clay

Percent silt-clay by volume was well below 1% for all samples, with a range of 0 to 0.09% and mean of $0.01 \pm 0.003\%$. However, we did see variation with respect to treatment (KW $p = 0.011$; $R > C$, $p = 0.012$) and intertidal zone (KW $p = 0.045$; high $>$ low, $p = 0.03$), but not sampling time. In the high intertidal zone, samples from the renourished sites had significantly higher percentages than those from the control sites ($p = 0.002$; Table 1). Percent silt-clay in low intertidal samples did not vary with respect to treatment, but did vary with respect to sampling time ($p = 0.003$), with significantly lower percentages at all subsequent sampling times compared to 3 days post-renourishment (June) ($p < 0.03$; Supplementary Fig. 2).

Percent Shell Hash

Percent shell hash by volume ranged from 0 to 6.37% with an overall mean of $1.13 \pm 0.28\%$. Percent shell hash varied with respect to treatment (KW $p < 0.0001$; $R > C$, $p < 0.0001$) and intertidal zone ($p = 0.039$; high $>$ low, $p = 0.041$), but did not vary significantly with respect to sampling time. In the high intertidal, percent shell hash varied with respect to treatment ($p = 0.0001$; $R > C$, $p = 0.0001$; Table 1), but not sampling time (Supplementary Fig. 2a). Percent shell hash did not vary at the low intertidal between treatments or among sampling times (Table 1; Supplementary Fig. 3b and c).

Sorting

σ_1 ranged from 0.44 (well-sorted) to 0.96Φ (moderately well-sorted) with a mean of $0.63 \pm 0.02\Phi$. σ_1 varied with respect to treatment ($p = 0.0004$), but not intertidal zone (high, low) or sampling time (Supplementary Fig. 4a). Post hoc comparisons showed that the renourished treatment was more poorly sorted compared to the control ($p = 0.0004$; Table 1). At the high intertidal zone only, σ_1 varied with respect to site ($p = 0.002$): C1 was more poorly sorted compared to C2 ($p = 0.02$), but both renourished sites were more poorly sorted compared to C1 and C2 ($p < 0.05$; Supplementary Fig. 4b). The low intertidal zone varied with respect to sampling time

($p = 0.04$), with sediment 230 days post-renourishment being more poorly sorted than that from 36 days post-renourishment ($p = 0.03$; Supplementary Fig. 4c).

High-Throughput DNA Sequencing

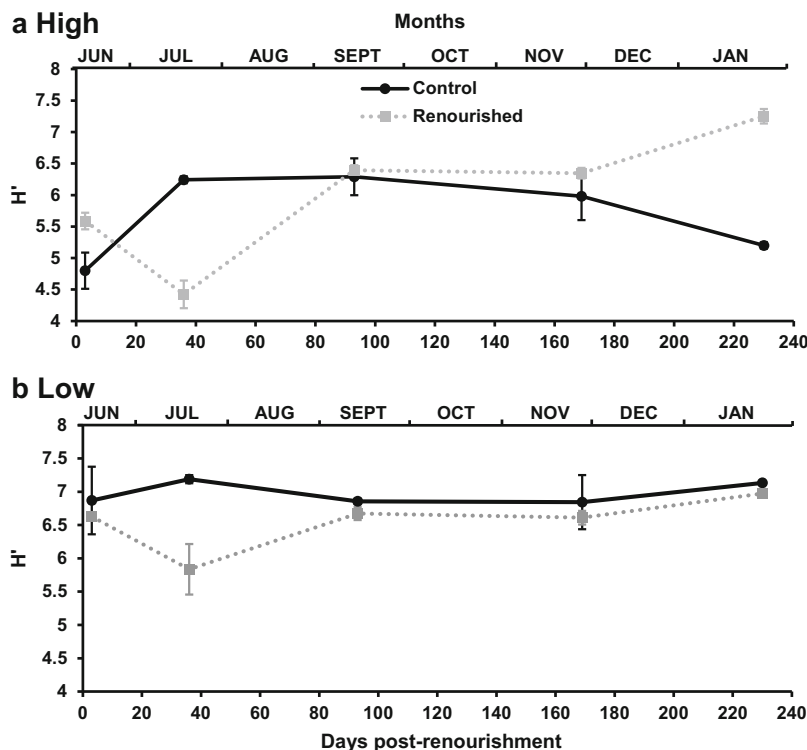
A total of 473,622 raw reads from 40 total samples were generated. After quality and size filtering, 282,480 sequences remained with an average sequence length of 462 bp. After removal of chimeras and singletons, 201,898 reads remained with an average of 5047 ± 436 reads per sample. Data were rarefied to 1614 sequences per sample for subsequent alpha and beta diversity analyses.

Alpha Diversity

H' , S , and Chao1 varied significantly with respect to intertidal zone (high and low; KW $p < 0.001$), with low intertidal samples being more diverse than those from the high intertidal ($p < 0.001$ for all metrics; Supplementary Table 2). E also varied significantly, but by treatment ($p = 0.020$), with the control being more even than the renourished overall ($p = 0.021$; Supplementary Table 2).

In the high intertidal zone, the control treatment had marginally higher evenness compared to the renourished treatment ($p < 0.10$; Supplementary Table 2). S and Chao1 also varied marginally by sampling time ($p < 0.10$): there was higher diversity and richness in both treatments at day 93 (September) compared to day 3 (June) and 36 (July) days post-renourishment (Fig. 6a). In fact, the renourished treatment maintained higher species diversity from day 93 to the end of the sampling period compared to the control and had greater diversity and evenness in samples collected in January 2015 (230 days post-renourishment) compared to those collected at 36 days post-renourishment in July 2014 ($p < 0.05$ for both; Fig. 6a). In the low intertidal, H' and E varied by treatment, with sediments from the control being more diverse and more even than the renourished treatment ($p = 0.026$, 0.064 , resp.; Supplementary Table 2; Fig. 6b). When examining each treatment separately, H' , S , and Chao1 for the control samples varied with respect to intertidal zone ($p < 0.001$). The low intertidal was significantly more diverse than the high

Fig. 6 Shannon-Weiner diversity (H') in sediment collected from the control and renourished treatments from **a** the high intertidal zone and **b** the low intertidal zone from June 2014 to January 2015. Error bars represent standard error



throughout the sampling period ($p < 0.001$; Supplementary Table 2). These differences in diversity between intertidal zones were not evident for the renourished treatment, where H' and E varied only by sampling time ($p < 0.05$).

Beta Diversity

ANOSIM based on unweighted and weighted UniFrac distances were qualitatively similar in that the R values differed slightly, but not in level of significance (data not shown). For simplicity, we chose to present the results based on unweighted distances here. ANOSIM revealed that the communities from both treatments (renourished and control) were indistinguishable overall, despite having a p value < 0.05 (Supplementary Table 3; Clarke and Gorley 2001). Communities from the high and low intertidal zones, however, were different from one another with some overlap (Fig. 7; Supplementary Table 3).

Examining samples from only the high intertidal zone revealed a difference in community structure between renourished and control samples and among communities from different sampling times (Supplementary Table 3; Fig. 7). Immediately following renourishment (days 3 and 36 in June and July, resp.), the communities from the renourished treatment were similar to the control sites from all sampling times (Supplementary Table 3, Fig. 7). Communities from the high intertidal renourished sites from later sampling dates (93, 169, and 230 days post-renourishment in September 2014, November 2014, and January 2015, resp.), however, differed from all other samples

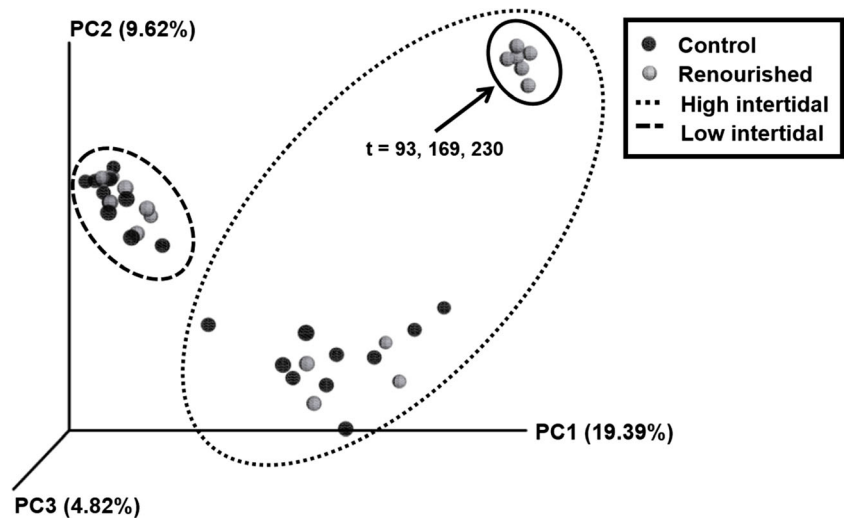
collected from the high intertidal zone, but were similar to one another (Supplementary Table 3, Fig. 7).

At the low intertidal zone, there were only differences in community structure among sampling times (Supplementary Table 3). The PCoA plot of samples collected only at the low intertidal zone (Supplementary Fig. 5) showed that the communities from later sampling times (169 and 230 days post-renourishment in November 2014 and January 2015, resp.) appear to be more similar to the communities collected from those same times than those from the earlier sampling times (3, 36, 93 days post-renourishment in June, July, and September 2014, resp.), regardless of treatment.

Taxonomy

Ochrophyta (composed primarily of diatoms (Bacillariophyceae, Mediophyceae, and Diatomea)) dominated the communities at the control sites throughout the sampling period (31.5–51.9% relative abundance), while the dominant groups from the renourished sediments were more variable through time (Fig. 8). From the renourished samples, the greatest relative abundance of diatoms was at 3 days post-renourishment (30.7%) and was surprisingly comparable to the abundance found in control samples (31.5%; Fig. 8a). When examining each intertidal zone more closely, we found that diatoms were actually the dominant taxa in the high intertidal renourished sediment samples 3 days post-renourishment (52.3%), with a shift in dominance to Euamoebida 36 days post-renourishment (81.7%) and then to chlorophytes thereafter (57–87.4%; Fig. 8b). The

Fig. 7 Principal coordinate analysis (PCoA) plot based on unweighted UniFrac distances of samples collected from the renourished and control sites from the high and low intertidal zones from five sampling dates. Groupings are defined based on analysis of similarity results (Supplementary Table 3). Refer to Supplementary Fig. 5 to examine the PCoA plot of samples from the low intertidal zone only. t = days post-renourishment



high intertidal control sediment samples also showed a shift toward chlorophytes and ciliates, but not until 169 and 230 days post-renourishment, and diatoms were still at >14% relative abundance (compared to <2% at the renourished sites; Fig. 8b). The renourished low intertidal sediment samples also had more diatoms at 3 days compared to 36 days post-renourishment (14.7 vs. 24.7%), with ciliates dominating these samples, but the relative abundance of diatoms increased thereafter—22.8% at 93 days, 28.2% at 169 days, and 40.3% at 230 days post-renourishment (Fig. 8c). A similar compositional pattern through time occurred in the low intertidal control samples, with the exception of 36 days post-renourishment when diatoms had a greater relative abundance compared to 3 days post-renourishment (52.7% vs. 26.9%).

Correlation Analyses

We found a significant and positive relationship between EPS and chl *a* at the control sites, but these variables were negatively correlated at the renourished treatments (Table 2). For both treatments, EPS and max erosion were significantly and positively correlated, and chl *a* and max erosion were significantly and negatively correlated (Table 2). Examining each intertidal zone separately, however, revealed that EPS and chl *a* were positively correlated at the low and mid intertidal zones, but were negatively correlated, though with marginal significance, at the high intertidal zone (Table 2).

Chl *a* and EPS were not significantly correlated with median grain size (Supplementary Table 4). Overall, well-sorted sediment had more chl *a*, and sediments that had a higher percentage of shell hash and silt-clay had less chl *a* (Supplementary Table 4). EPS, however, was positively correlated with percent shell hash and percent silt-clay (Supplementary Table 4). More poorly sorted sediment had higher max erosion, and sediments with higher percentages of shell hash and silt-clay had less max erosion (Supplementary Table 4).

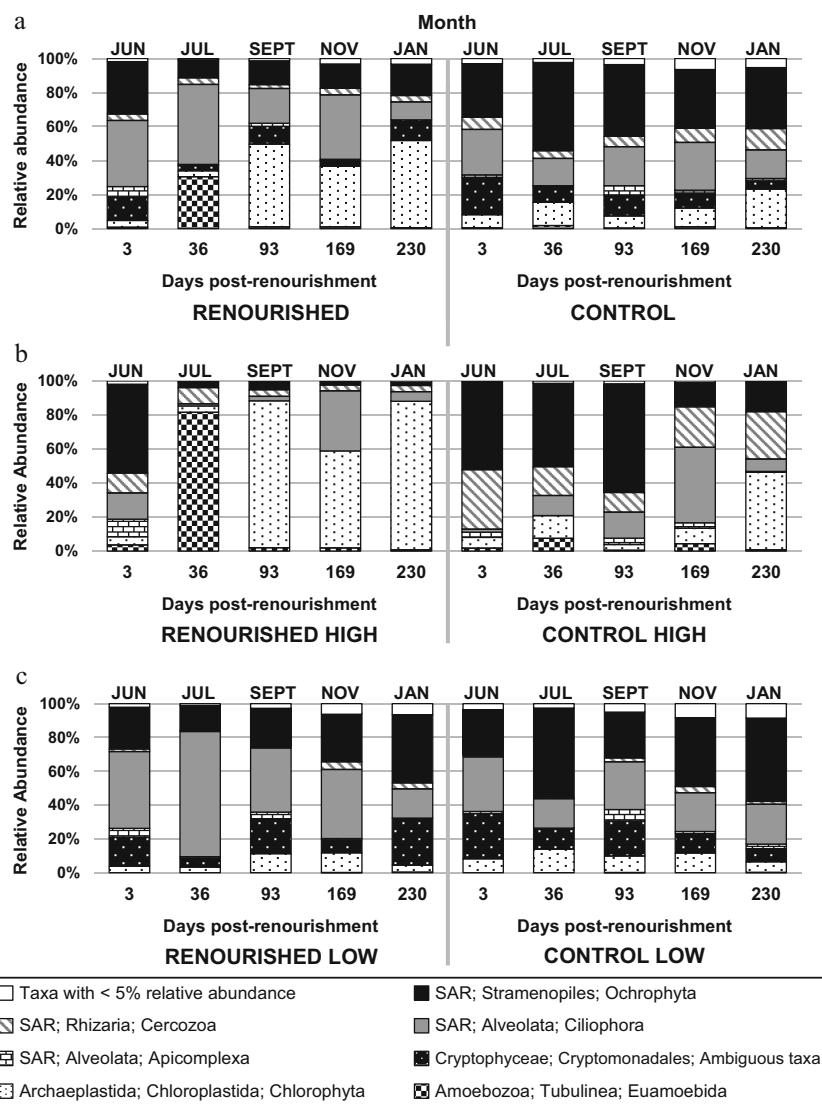
H' , S , and Chao1 were significantly and positively correlated with chl *a* at the control sites, with Chao1 also being positively correlated with chl *a* in sediments from the renourished sites (Supplementary Table 5). H' , S , and Chao1 were negatively correlated with EPS at the control sites with Chao1 being negatively correlated with EPS sampled from the renourished sites (Supplementary Table 5). More max erosion was associated with higher diversity indices in sediments from the control, but not the renourished treatment (Supplementary Table 5). Max erosion and wind speed were positively correlated in the mid (Spearman's $\rho = 0.48$, $p = 0.02$), but not in the other intertidal zones (Supplementary Fig. 6).

We found that sediment temperature was significantly higher within the high intertidal compared to the low intertidal zone overall ($p = 0.009$) and saw significant correlations between diversity and sediment temperature overall and at the renourished sites (Supplementary Table 5). H' and sediment temperature were negatively correlated at both treatments, and S and Chao1 were strongly and negatively correlated with sediment temperature at the renourished sites (Supplementary Table 5). Correlations with respect to most granulometric measurements were not significant.

Discussion

Our first goal was to examine the recovery of BMA biomass within the intertidal zone after a beach renourishment event in Folly Beach, SC. Our data suggest that renourishment may affect the seasonal pattern of BMA chl *a*, thereby affecting the amount of primary production available in the ecosystem. We also found differences between the intertidal zones—with higher biomass at the low and mid intertidal zones compared to the high. Surprisingly, chl *a* in sediments from the renourished sites immediately following renourishment were comparable to that of the control. Cahoon et al. (2012) also did

Fig. 8 Bar charts summarizing the relative abundance of taxa found in samples collected from the renourished and control sites (a), from the high intertidal zone (b), and from the low intertidal zone (c) from June 2014 to January 2015 (3 to 230 days post-renourishment). We excluded taxonomic groups with less than 5% relative abundance for clarity of the figure. Taxonomic level 4 of the SILVA v128 database (Quast et al. 2013) was used here to enable clear visualization of individual taxonomic groupings



not observe a reduction of chl *a* levels immediately following renourishment of Carolina Beach, North Carolina and hypothesized that the borrowed sediments used may have contained BMA initially. However, in our study, the levels at the control were also already very low in June and July, so this result

could be confounded with seasonality. We agree that the borrowed sediment could have contained BMA (or phytoplankton from the water column) thus resulting in similar chl *a* levels at both renourished and control sites. Despite the borrowed material coming from depth (8.8–13.4 m) where

Table 2 Spearman’s rank correlation coefficients (ρ) that were statistically significant ($p < 0.05$) or marginally significant ($p < 0.1$; in italics) for chlorophyll *a* (chl *a*), extracellular polymeric substances (EPS), maximum (max) erosion, and net erosion data when examining

all data (both treatments, three intertidal zones, and nine sampling dates), each treatment separately, and each intertidal zone separately. *n.s.* not statistically significant

Variable	By variable	All data ρ	Renourished ρ	Control ρ	High ρ	Mid ρ	Low ρ
Chl <i>a</i>	EPS	<i>n.s.</i>	-0.33	0.36	<i>-0.23</i>	0.43	0.50
	Max erosion	-0.65	-0.74	-0.52	-0.41	<i>n.s.</i>	<i>-0.22</i>
	Net erosion	<i>n.s.</i>	-0.38	<i>n.s.</i>	0.33	0.29	<i>n.s.</i>
EPS	Max erosion	0.52	0.63	0.28	0.28	0.35	<i>n.s.</i>
	Net erosion	0.26	0.42	<i>n.s.</i>	<i>n.s.</i>	<i>n.s.</i>	0.40
Max erosion	Net erosion	0.44	0.57	0.34	-0.30	0.65	0.56

there is less light available, BMA are known to be present and productive in surface sediments (0–0.5-cm deep) from the South Atlantic Bight off Georgia and Florida at depths up to 40 m (Nelson et al. 1999). Ideally, we would have sampled the borrowed sediment or been able to sample as soon as the sediment was deposited on the beach face (as opposed to ~3 days post-renourishment), but logistical constraints precluded this. Contrary to Cahoon et al. (2012), we did observe a delay in a seasonal peak of chl *a* in mid-summer by approximately a month at the renourished sites, with indication of recovery only after 93 days in September when chl *a* levels between sediments from the renourished and control sites were again comparable.

When exploring each of the high, mid, and low intertidal zones separately, data from both the low and mid intertidal zones suggested that recovery of biomass may not have occurred until November (169 days post-renourishment), though unfortunately again this may be confounded with the natural decline of chl *a* as summer turns to fall. Sediments from the high intertidal zone had less chl *a* compared to sediments from the mid and low zones regardless of treatment, and seasonal trends were not easily discernable—the control sites peaked in August and November, but negligibly. In a previous study, BMA biomass was found to be inversely proportional to the length of time sediment was immersed (van der Wal et al. 2010), so it was surprising that we found less chl *a* in sediments from the high intertidal zone where tidal inundation occurred only with very large tides. While median grain size was not significantly larger at the high intertidal zone compared to the low, percentage of shell hash was greater, and lower biomass has been associated with coarser sediments (Miller et al. 1996; Cahoon et al. 2012, 1999). We did not see a significant correlation between chl *a* and grain size nor did grain size vary by intertidal zone. This indicates that perhaps other factors that we did not measure (e.g., nutrient supply, grazing pressure) may have affected the differences in recovery times among intertidal zones.

Because of the raised elevation of the renourished beach face, a steep, ~0.5-m berm developed just below the mid intertidal zone shortly following renourishment. This berm prevented tidal inundation of the mid and high intertidal renourished sites for several months following renourishment. The eventual breakdown of the berm resulted in more regular tidal inundation at the mid, and later, the high intertidal zone. The delay in tidal inundation corresponded roughly to the patterns in recovery we saw in terms of chl *a*: the low intertidal zone recovered more quickly, followed by the mid, and then by the high intertidal zone. The halting of tidal inundation did not appear to affect chl *a* differences between the renourished and control high intertidal zone sites, but it may have contributed to differences we saw in community structure. It appears that the communities that repopulated the high intertidal zone quickly (or were already in the borrowed sediment) in June

and July were more similar to the control than the communities that were present in the renourished high intertidal zone later on in September, November, and January. In fact, we saw that the relative abundance of taxa present 3 days post-renourishment was similar between the control and renourished sites. Overall, diatoms were dominant in control samples throughout the entire sampling period, with some seasonal changes, but chlorophytes and ciliates became the dominant groups found at the renourished sites 93, 169, and 230 days post-renourishment. This shift in dominant taxa was mainly due to changes in the communities found in the high intertidal zone; while the renourished, low intertidal zone also had fewer diatoms at 36 days compared to 3 days post-renourishment, the communities appeared to recover by 230 days post-renourishment, with diatoms becoming the dominant taxa. This alteration in high intertidal communities could be the result of having little to no tidal inundation for months following renourishment. Therefore, artificially elevating the beach may be more detrimental to BMA communities than the burial of extant communities or changes in sediment. Further, renourishment may not immediately affect BMA community structure as might be expected, but rather the effects may be seen months after the disturbance.

Intertidal zonation patterns from high to low shore are common for a variety of organisms, and we found this to be true with BMA community structure as well. Overall, we saw striking differences between the high and low intertidal BMA communities. These differences are most likely due to the different physical environmental conditions experienced at the high and low intertidal zones under normal circumstances, and in our case, these differences were further exacerbated by the formation of the berm at the renourished sites. Different species of diatoms, for instance, demonstrate differential sensitivity to tidal exposure and substratum (Sherrod 1999; Weckström and Juggins 2005). We also found that diversity was higher and communities were more even in sediments from the low intertidal zone compared to those from the high throughout the duration of our sampling, but only at the control sites. At the renourished sites, communities from both the low and high intertidal zones were similar with respect to diversity and evenness and only varied temporally; diversity decreased immediately following renourishment in June to July and then steadily increased from July 2014 to January 2015. This pattern was not evident at the control sites. Therefore, it appears that while BMA communities from the renourished sites were able to recover in terms of diversity, renourishment appeared to disrupt the natural differences in communities among intertidal zones. For BMA communities found in the low intertidal zone, there appeared to be no compositional differences between the renourished and control sites, but rather significant changes through time, which appear to be seasonal. The low intertidal BMA communities endure resuspension with near-continuous tidal inundation

and thus may be less impacted by renourishment and/or recover more quickly than communities further inshore.

The direct relationship between diversity and richness and biomass that we saw overall and in samples from the control sites was as expected. This relationship has been documented for natural diatom communities from estuarine mudflats both in the field (Forster et al. 2006) and experimentally (Vanelslander et al. 2009). While we did not find a significant relationship between diversity and many of the granulometric measurements, we saw a significant negative relationship between chl *a* and the proportion of fine sediments (i.e., percent silt-clay). A previous study examining the effects of sediment grain size on BMA biomass found this same relationship across several estuaries in NC and MA, USA, and Manukau Harbour Estuary, New Zealand (Cahoon et al. 1999). In the current study, sediment from the renourished sites was more poorly sorted; it was composed of a higher percentage of shell hash and fine sediments compared to the control. It is possible that poor sorting resulted in less chl *a* and thereby lower diversity until reestablishment of the granulometric norms. However, sediment from the high intertidal renourished sites remained more poorly sorted than the control throughout and never seemed to recover, likely due to the formation of the berm and lack of tidal inundation. Species richness exceeded the control at these sites starting at 93 days post-renourishment, but the community shifted such that diatoms were $\leq 5\%$ relative abundance. These communities instead were dominated by chlorophytes and ciliates that were likely better adapted to the altered granulometric and hotter, drier conditions. This highlights the importance of using community composition as a metric of recovery as opposed to alpha diversity indices alone, as the latter can be misleading. Peterson and Bishop (2005) called attention to the fact that diversity indices are still being used to assess the impact of beach renourishment, though Nelson (1993) warned against their use, as the interpretations can be dubious.

Lastly, we examined the relationships among chl *a*, EPS, and erosion. One of the main purposes of renourishment is combating erosion, but because we know that BMA produce sediment-stabilizing EPS, we proposed that renourished sites would exhibit more erosion as an effect of reduced BMA. We expected EPS to be lower in renourished sediments immediately following renourishment, assuming that the borrowed sediment was near devoid of BMA, and gradually increase with the reestablishment of BMA communities. Instead, chl *a* and EPS in sediments from the renourished sites were comparable or exceeded that sampled from the control sites initially, and further, neither EPS nor max erosion varied by treatment. We also expected to see a strong, positive correlation between chl *a* and EPS and a strong, negative correlation between EPS and max erosion based on previous studies done in estuarine systems (e.g., Underwood et al. 1995, Underwood & Smith 1998, Yallop et al. 2000). Chl *a* from control samples

was positively correlated with EPS, but we found an inverse relationship between EPS and chl *a* in samples taken from the renourished sites. Bacteria present in borrow sediment, whose biomass was unaccounted for, may have contributed to EPS production and sediment stabilization. Their presence could explain the lack of variation in EPS and max erosion between sites and the inverse relationship between EPS and chl *a* at the renourished site. Non-BMA EPS producers in renourished sediments could also explain why an inverse correlation between EPS and max erosion was observed, as expected, at both control and renourished sites. Alternatively, some of our EPS data were at or below the detection limit of the assay, which may have affected our abilities to accurately quantify EPS. In lower energy environments, like those in Charleston Harbor, chl *a* concentrations in the summer have been reported to be $\sim 3\text{--}7\text{-}\mu\text{g g}^{-1}$ dry sediment in sandy sediments and $\sim 7\text{--}10\text{-}\mu\text{g g}^{-1}$ dry sediment in muddy sediments (Plante et al. 2016). Our concentrations did not exceed $2\text{-}\mu\text{g g}^{-1}$ dry sediment throughout the sampling period at either treatment. Therefore, the role of EPS as a sediment stabilizer is likely not as important in energetic, sandy sites such as Folly Beach, because of lower biomass (and thus lower EPS production) and higher erosion compared to lower-energy sites.

The study design for most renourishment experiments and projects are wrought with issues (Peterson and Bishop 2005), and the present study also has its limitations. Ideally, the sampling sites would have been similarly spaced and the control sites would be further away from the renourished zone, but unfortunately site selection was largely out of our control. For most analyses, however, the data collected from the two sites from each treatment were similar enough to combine, so the spatial differences appeared to be negligible. Being constrained to these certain sites however did prevent us from being able to collect from existing sediment prior to renourishment, and as mentioned above, sampling immediately following renourishment (instead of 3–5 days post-renourishment). We also acknowledge that using chl *a* for estimating biomass has its limitations; chl *a* can vary based on environmental conditions (e.g., light, temperature, nutrients, grazing pressure) and BMA cell size and community composition (Baulch et al. 2009). This method is commonly used because of its ease and low cost, however, and thus is still relevant for comparison to other studies. Furthermore, HTS has its constraints with regard to characterizing communities. We used primers that were designed to amplify diatom DNA, but found that these also amplified DNA of metazoan and fungal taxa. The primers we used also do not differentiate between benthic and planktonic forms, so it is possible that the differences found between the intertidal zones were augmented due to the increased likelihood of plankton “contaminating” low intertidal sediments. More specific PCR primers and more specific databases for taxonomic assignment would be helpful for future studies.

Conclusions

It appears that artificially elevating the beach face, which can prevent regular tidal immersion, may have more of a long-term impact on BMA communities than the initial burial of existing communities. We saw the development of a steep berm at the renourished sites, which seemed to shape when and how BMA recovered in terms of biomass and community structure.

Recovery of BMA biomass appeared to occur between 93 and 169 days post-renourishment in the intertidal zone of Folly Beach, SC. Biomass recovered in sequence from the low to the high intertidal zone—a sequence that roughly corresponded to when each experienced more frequent tidal inundation due to the eventual breakdown of the berm. Renourishment also disturbed the natural intertidal zonation of BMA communities from the low to high intertidal zone. Further, the community structure within the high intertidal zone was only ever comparable to the control immediately following renourishment, i.e., communities here still had not recovered ~7 months after renourishment. Compositional changes in primary producers can result in changes in nutrient cycling and this can have cascading effects on upper trophic levels. While our study provides some evidence that EPS may be important to stabilizing sediment on high-energy beaches, it is likely unrelated to BMA in particular, and additional studies, using a more sensitive EPS assay, are needed in order to better understand its importance in high-energy environments. Beach renourishment will likely become increasingly prevalent as a means to mitigate beach erosion as sea levels rise and storm frequencies increase due to climate change. Thus, information about the effects of renourishment on the primary producers of coastal ecosystems is crucial.

Acknowledgments We thank the Great Lakes Dredge and Dock Company and the US Army Corps of Engineers for providing access to field sites. We also thank Jennifer Ness at the National Institute of Standards and Technology's Material Measurement Laboratory for providing training on the Malvern Mastersizer 3000 for particle size analyses and the Hollings Marine Laboratory for access to the facility. Morgan Larimer and Caroline Cooper provided both laboratory and field assistance. Kevin Spanik, Stacy Krueger-Hadfield, Meredith Smylie, Nathan Butcher, and Paige Bippus also provided field assistance. This is Grice Marine Laboratory publication 511.

Funding Information This work was funded by a Summer Research with Faculty (SURF) grant at The College of Charleston, Charleston, SC. We would also like to acknowledge the Proteogenomics Facility supported by the National Institutes of Health Grants (P30GM103342, P20GM103499) and MUSC's Office of the Vice President for Research.

Compliance with Ethical Standards

Conflict of Interest The authors declare that they have no conflict of interest.

References

- Baulch, H.M., M.A. Turner, D.L. Findlay, R.D. Vinebrooke, and W.F. Donahue. 2009. Benthic algal biomass—Measurement and errors. *Canadian Journal of Fishers and Aquatic Sciences*. 66 (11): 1989–2001.
- Bézy, V.S., R.A. Valverde, and C.J. Plante. 2014. Olive ridley sea turtle hatching success as a function of microbial abundance and the microenvironment of in situ nest sand at Ostional, Costa Rica. *Journal of Marine Biology*. 2014: 1–10. <https://doi.org/10.1155/2014/351921>.
- Cahoon, L.B., J.E. Nearhoof, and C.L. Tilton. 1999. Sediment grain size effect on benthic microalgal biomass in shallow aquatic ecosystems. *Estuaries* 22 (3): 735–741.
- Cahoon, L.B., E.S. Carey, and J.E. Blum. 2012. Benthic microalgal biomass on ocean beaches: Effects of sediment grain size and beach renourishment. *Journal of Coastal Research* 28: 853–859.
- Caporaso, J.G., J. Kuczynski, J. Stombaugh, K. Bittinger, F.D. Bushman, E.K. Costello, N. Fierer, A.G. Pena, J.K. Goodrich, J.I. Gordon, G.A. Huttley, S.T. Kelley, D. Knights, J.E. Koenig, R.E. Ley, C.A. Lozupone, D. McDonald, B.D. Muegge, M. Pirrung, J. Reeder, J.R. Sevinsky, P.J. Turnbaugh, W.A. Walters, J. Widmann, T. Yatsunenko, J. Zaneveld, and R. Knight. 2010a. QIIME allows analysis of high-throughput community sequencing data. *Nature Methods* 7 (5): 335–336.
- Caporaso, J.G., K. Bittinger, F.D. Bushman, T.Z. DeSantis, G.L. Andersen, and R. Knight. 2010b. PyNAST: A flexible tool for aligning sequences to a template alignment. *Bioinformatics* 26 (2): 266–267.
- Chao, A. 1984. Non-parametric estimation of the number of classes in a population. *Scandinavian Journal of Statistics* 11: 265–270.
- City of Folly Beach. 2015. 2015 local comprehensive beach management plan. 131 pp. <https://www.scdhec.gov/sites/default/files/docs/HomeAndEnvironment/Docs/State-ApprovedLCBMP.pdf>. Accessed 21 Sept 2018.
- Clarke, K.R. 1993. Non-parametric multivariate analysis of changes in community structure. *Australian Journal of Ecology* 18 (1): 117–143.
- Clarke, K.R., and R.N. Gorley. 2001. *PRIMER v5: User manual/tutorial*. Plymouth: PRIMER-E.
- Decho, A.W. 1990. Microbial exopolymer secretions in ocean environments: Their role(s) in food webs and marine processes. *Oceanography and Marine Biology: An Annual Review* 28: 73–153.
- Edgar, R.C. 2010. Search and clustering orders of magnitude faster than BLAST. *Bioinformatics* 26 (19): 2460–2461.
- Edgar, R.C., B.J. Haas, J.C. Clemente, C. Quince, and R. Knight. 2011. UCHIME improves sensitivity and speed of chimera detection. *Bioinformatics* 27 (16): 2194–2200.
- Folk, R.L., and W. Ward. 1957. Brazos River bar: A study in the significance of grain size parameters. *Journal of Sedimentary Petrology* 27 (1): 3–26.
- Forster, R.M., V. Créach, K. Sabbe, W. Vyverman, and L.J. Stal. 2006. Biodiversity-ecosystem function relationship in microphytobenthic diatoms of the Westerschelde estuary. *Marine Ecology Progress Series* 311: 191–201.
- Heip, C. 1974. A new index measuring evenness. *Journal of the Marine Biological Association of the United Kingdom* 54 (03): 555–557.
- Hernandez, R.J., Y. Hernandez, N.H. Jimenez, A.M. Piggot, J.S. Klaus, Z. Feng, A. Reniers, and H.M. Solo-Gabriele. 2014. Effects of full-scale beach renovation on fecal indicator levels in shoreline sand and water. *Water Research* 48: 579–591.
- Holland, A.F., R.G. Zingmark, and J.M. Dean. 1974. Quantitative evidence concerning the stabilization of sediments by marine benthic diatoms. *Marine Biology* 27 (3): 191–196.

- Levine, N., C. Kaufman, M. Katuna, S. Harris, and M. Colgan. 2009. Folly Beach, South Carolina: An endangered barrier island. In Kelley, J.T., O.H. Pilkey, J.A.G. Cooper, eds., *America's most vulnerable coastal communities: Geological society of america special paper 460*, p. 91–110. [https://doi.org/10.1130/2009.2460\(06\)](https://doi.org/10.1130/2009.2460(06)).
- Lozupone, C., and R. Knight. 2005. UniFrac: A new phylogenetic method for comparing microbial communities. *Applied and Environmental Microbiology* 71 (12): 8228–8235.
- Lubarsky, H.V., C. Hubas, M. Chocholek, F. Larson, W. Manz, D.M. Paterson, and S.U. Gerbersdorf. 2010. The stabilization potential of individual and mixed assemblages of natural bacteria and microalgae. *PLoS One* 5 (11). <https://doi.org/10.1371/journal.pone.0013794>.
- Luddington, I.A., I. Kaczmarek, and C. Lovejoy. 2012. Distance and character-based evaluation of the V4 region of the 18S rRNA gene for the identification of diatoms (Bacillariophyceae). *PLoS One* 7 (9). <https://doi.org/10.1371/journal.pone.0045664>.
- MacIntyre, H.L., R.J. Geider, and D.C. Miller. 1996. Microphytobenthos: The ecological role of the "secret garden" of unvegetated, shallow-water marine habitats. I. Distribution, abundance and primary production. *Estuaries and Coasts* 19 (2): 186–201.
- Madsen, K.N., P. Nilsson, and K. Sundbäck. 1993. The influence of benthic microalgae on the stability of a subtidal sediment. *Journal of Experimental Marine Biology and Ecology* 170 (2): 159–177.
- McLachlan, A., T. Wooldridge, and A.H. Dye. 1981. The ecology of sandy beaches in southern Africa. *South African Journal of Zoology* 16 (4): 219–231.
- Miller, D.C., R.J. Geider, and H.L. MacIntyre. 1996. Microphytobenthos: The ecological role of the "Secret Garden" of unvegetated, shallow-water marine habitats. II. Role in sediment stability and shallow-water food webs. *Estuaries* 19 (2): 202–212.
- Nelson, W.G. 1993. Beach restoration in the southeastern US: Environmental effects and biological monitoring. *Ocean and Coast Management* 19 (2): 157–182.
- Nelson, J.R., J.E. Eckman, C.Y. Robertson, R.L. Marinelli, and R.A. Jahnke. 1999. Benthic microalgal biomass and irradiance at the sea floor on the continental shelf of the South Atlantic Bight: Spatial and temporal variability and storm effects. *Continental Shelf Research* 19 (4): 477–505.
- Nilsson, C. 1995. Microbenthic communities with emphasis on algal-nutrient relations. PhD dissertation. Göteborg, Sweden: Göteborg University.
- Peterson, C.H., and M.J. Bishop. 2005. Assessing the environmental impacts of beach nourishment. *BioScience* 55 (10): 887–896.
- Plante, C.J., V. Fleer, and M.L. Jones. 2016. Neutral processes and species sorting in benthic microalgal community assembly: Effects of tidal resuspension. *Journal of Phycology* 52 (5): 827–839.
- Price, M.N., P.S. Dehal, and A.P. Arkin. 2010. FastTree 2—Approximately maximum-likelihood trees for large alignments. *PLoS One*. <https://doi.org/10.1371/journal.pone.0009490>.
- Quast, C., E. Pruesse, P. Yilmaz, J. Gerken, T. Schweer, P. Yarza, J. Peplies, and F.O. Glöckner. 2013. The SILVA ribosomal RNA gene database project: Improved data processing and web-based tools. *Nucleic Acids Research* 41: 590–596.
- R Core Team. 2013. *R: A language and environment for statistical computing*. Vienna: R Foundation for Statistical Computing <http://www.R-project.org/>.
- Sherrod, B.L. 1999. Gradient analysis of diatom assemblages in a Puget Sound salt marsh: Can such assemblages be used for quantitative paleoecological reconstructions? *Palaeogeography, Palaeoclimatology, Palaeoecology* 149 (1–4): 213–226.
- Snigirova, A. 2013. Benthic microalgae under the influence of beach nourishment in the Gulf of Odessa (the Black Sea). *Botanica Lithuanica* 19 (2): 120–128.
- Sousa, E.C.P.M., and C.J. David. 1996. Daily variation of microphytobenthos photosynthetic pigments in Aparecida Beach-Santos (23° 58' 48" S, 46° 19' 00" W), Sao Paulo, Brazil. *Revista Brasileira de Biologia* 56: 147–154.
- Speybroeck, J.D., D. Bonte, W. Courtens, T. Gheskiere, P. Grootaert, J. Maelfait, M. Mathys, S. Provoost, K. Sabbe, E.W.M. Stienen, V. van Lancker, M. Vincx, and S. Degraer. 2006. Beach nourishment: An ecologically sound coastal defense alternative? A review. *Aquatic Conservation* 16 (4): 419–435.
- Stal, L.J. 2010. Microphytobenthos as a biogeomorphological force in intertidal sediment stabilization. *Ecological Engineering* 36(2): 236–245.
- Steele, J.H., and I.E. Baird. 1968. Production ecology of a sandy beach. *Limnology and Oceanography* 13: 14–25.
- Thistle, D., G.L. Weatherly, and S.C. Ertman. 1995. Shelf harpacticoid copepods do not escape into the seabed during winter storms. *Journal of Marine Research* 53 (5): 847–863.
- Tolhurst, T.J., B. Jesus, V. Brotas, and D.M. Paterson. 2003. Diatom migration and sediment armouring—An example from the Tagus Estuary, Portugal. *Hydrobiologia* 503 (1–3): 183–193.
- Underwood, G.J.C., and J. Kromkamp. 1999. Primary production by phytoplankton and microphytobenthos in estuaries. *Advances in Ecological Research* 29: 93–153.
- Underwood, G.J.C., and D.J. Smith. 1998. Predicting epipellic diatom exopolymer concentrations in intertidal sediments from sediment chlorophyll *a*. *Microbial Ecology* 35: 116–125.
- Underwood, G.J.C., D.M. Paterson, and R.J. Parkes. 1995. The measurement of microbial carbohydrate exopolymers from intertidal sediments. *Limnology and Oceanography* 40 (7): 1243–1253.
- USACE. 2013. Environmental assessment draft, Folly Beach shore protection project and use of outer continental shelf sand, Charleston County, SC. 160 pp. <http://www.sac.usace.army.mil/Portals/43/docs/civilworks/nepadocuments/FollyBeachRenourishmentDraftEA2013-withAppendices.pdf>. Accessed 21 September 2018.
- Valverde, H.R., A.C. Trembanis, and O.H. Pilkey. 1999. Summary of beach nourishment episodes on the U.S. East Coast barrier islands. *Journal of Coastal Research* 15: 1100–1118.
- van der Wal, D., A. Wielemaker-van den Dool, and P.M.J. Herman. 2010. Spatial synchrony in intertidal benthic algal biomass in temperate coastal and estuarine ecosystems. *Ecosystems* 13: 338–351.
- Vanelslander, B., A. de Wever, N. van Oostende, P. Kaewnuratchadasorn, P. Vanormelingen, F. Hendrickx, K. Sabbe, and W. Vyverman. 2009. Complementarity effects drive positive diversity effects on biomass production in experimental benthic diatom biofilms. *Journal of Ecology* 97 (5): 1075–1082.
- Vázquez-Baeza, Y., M. Pirrung, A. Gonzalez, and R. Knight. 2013. EMPERor: A tool for visualizing high-throughput microbial community data. *GigaScience* 2 (1): 16.
- Wang, Q., G.M. Garrity, J.M. Tiedje, and J.R. Cole. 2007. Naive Bayesian classifier for rapid assignment of rRNA sequences into the new bacterial taxonomy. *Applied and Environmental Microbiology* 73 (16): 5261–5267.
- Weckström, K., and S. Juggins. 2005. Coastal diatom-environment relationships from the Gulf of Finland, Baltic Sea. *Journal of Phycology* 42: 21–35.
- Welschmeyer, N.A. 1994. Fluorometric analysis of chlorophyll *a* in the presence of chlorophyll *b* and phaeopigments. *Limnology and Oceanography* 39 (8): 1985–1992.
- Yallop, M.L., D.M. Paterson, and P. Wellsbury. 2000. Interrelationships between rates of microbial production, exopolymer production, microbial biomass, and sediment stability in biofilms of intertidal sediments. *Microbial Ecology* 39 (2): 116–127.
- Zimmermann, J., R. Jahn, and B. Gemeinholzer. 2011. Barcoding diatoms: Evaluation of the V4 subregion on the 18S rRNA gene, including new primers and protocols. *Organisms Diversity & Evolution* 11 (3): 173–192.